TECHNISCHE
UNIVERSITÄT
MÜNCHEN

INSTITUT FÜR INFORMATIK

Sonderforschungsbereich 342:
Methoden und Werkzeuge für die Nutzung
paralleler Rechnerarchitekturen

Sparse Grids: Applications to Multi-dimensional Schrödinger Problems

Sascha Hilgenfeldt, Robert Balder, Christoph Zenger

TUM-I9507
SFB-Bericht Nr.342/05/95 A
März 1995

TUM–INFO–03-95-I07-350/1.–FI

Anforderungen an: Prof. Dr. A. Bode
Sprecher SFB 342
Institut für Informatik
Technische Universität München
Arcisstr. 21 / Postfach 20 24 20
D-80290 München, Germany

Druck: Fakultät für Informatik der
Technischen Universität München

Sparse Grids: Applications to Multi-dimensional Schrödinger Problems

Sascha Hilgenfeldt
Robert Balder
Christoph Zenger
Institut für Informatik
Technische Universität München
Arcisstrasse 21, D-80290 München

March 1995

Abstract

Sparse grid methods applied to solve partial differential equations allow for a substantial reduction of numerical effort (to obtain equal error magnitudes) compared to conventional finite element methods. A short introduction to this new approach is given. Using a Ritz-Galerkin method on rectangular sparse grids, stationary Schrödinger equations of dimensionality $D \geq 2$ are solved numerically for a number of generic problems and the results are compared to exact values, perturbative results, and numerical computations of other authors. For problems with oscillator potentials (harmonic or anharmonic), the accuracy of eigenvalues for similar numbers of grid points and equal order of basis functions is increased by up to two orders of magnitude with respect to conventional FEM. Good solutions are obtained for singular potentials (hydrogen atom and hydrogen molecular ion), where the sparse grid was automatically refined using a local adaptation strategy. Schrödinger problems of high dimensionality (up to $D = 8$) become tractable with this algorithm, regardless of symmetries or separabilities of the potential functions, i.e. similar accuracies are to be expected for arbitrary potentials. As an example of a physically significant and intrinsically high-dimensional problem, eigenstates of a spin boson coupling model were computed.

1 Overview

The aim of this work is to demonstrate the applicability and power of the sparse grid finite element method [2] for the solution of the stationary Schrödinger equation of nonrelativistic quantum mechanics. Section 2 will give a brief outline of the sparse grid method and its advantages over conventional finite element methods (FEM) currently in use. Some modifications of regular sparse grid algorithms will be described as they further improve the performance for Schrödinger problems. For more details on the sparse grid method, we refer the reader to earlier work [6, 7, 8].

The algorithms used to solve this equation and their implementation into a computer program are subject of section 3. Chapter 4 will display results of the numerical solution of various Schrödinger problems in comparison to the values obtained by conventional FEM, by other accurate numerics or, if possible, by analytical or perturbative methods. We study harmonic and anharmonic oscillator potentials, singular (Coulombic) problems (namely, the hydrogen atom and hydrogen molecular ion), and, as an example for an intrinsically high-dimensional application, a spin-boson coupling system of Schrödinger equations. The last section summarizes the results and discusses further possible improvements.

2 The Sparse Grid Finite Element Method

Numerical methods for the solution of partial differential equations are ubiquitous in physics as well as in other sciences. Recently, finite element methods (FEM) have proved to be flexible, dependable tools for various problems in such fields as technical mechanics, hydrodynamics, or atomic and molecular physics. In many cases they are superior to other algorithms with respect to numerical efficiency.

A new variant of FEM, the *sparse grid finite element method*, was developed in 1990 [2]. It allows for massive reduction of the amount of storage needed to solve a problem with given accuracy. After having proved useful for computations of solutions of Laplace's and Poisson's equations and of eigenstates of Helmholtz's equation (cf. [7], [8]), the sparse grid FEM is applied to the stationary Schrödinger equation in this work.

2.1 Outline of the Method

The sparse grid FEM uses a non-nodal set of hierarchical basis functions to approximate the solution to a given problem. The finite elements have very different support sizes and are arranged in a hierarchical scheme which induces a tree data structure (cf. [8] and section 2.3.1 below). It was rigorously shown in [7] that for approximations of sufficiently smooth functions the hierarchical functions with small support volumes become increasingly unimportant. Precisely these elements, however, constitute the largest number of basis functions, i.e. the largest subset of the approximation space.

The sparse grid method reduces the dimension of the approximation space by eliminating all elements with supports smaller than a given value. Thus, the number of basis points is vastly decreased, especially if the problem is of high dimensionality. The remaining points form a *regular sparse grid*, as opposed to the conventional *full grid* (cf. Fig. 1).

2.2 Advantages of Sparse Grids

One might worry that this truncation of the approximation space will result in a corresponding loss in accuracy of the approximation. However, under

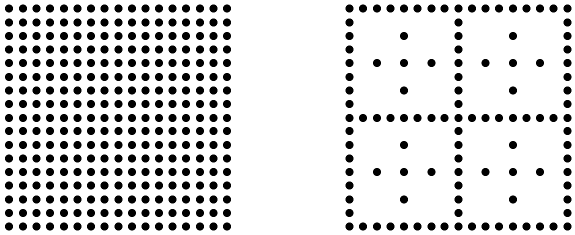

Figure 1: Full grid (left) and corresponding sparse grid (right).

weak conditions on the solution of the problem it can be shown that this is not the case. Namely, if a D-dimensional integration domain is discretized with mesh width h, the conventional (full) grid of a FEM contains $O(h^{-D})$ points, whereas the sparse grid has only $O(h^{-1}(\log(h^{-1}))^{D-1})$ nodes. If piecewise linear basis functions are chosen (like in this work), the full grid approximates the solution with $O(h^{-2})$ accuracy, while with sparse grids accuracy only decreases by a logarithmic factor to $O(h^{-2}(\log(h^{-1}))^{D-1})$. These results are summarized in table 1.

	full grid	sparse grid
# of nodes	$O(h^{-D})$	$O(h^{-1}(\log(h^{-1}))^{D-1})$
accuracy of approximation	$O(h^{-2})$	$O(h^{-2}(\log(h^{-1}))^{D-1})$

Table 1: Complexities and approximation accuracies of full and sparse grids.

Consequently, for $D \geq 2$ sparse grids show much better performance than full grids with the same amount of nodes. The advantages become more and more pronounced as the dimension of the problem increases.

2.3 Modifications to regular Sparse Grid Algorithms

The regular sparse grids described so far can be made even more efficient by locally modifying their structure. We present two possibilities to reduce the numerical effort needed to approximate functions of non-uniform smoothness.

2.3.1 Adaptive Sparse Grids

Sparse grids can be shaped according to the needs of the specific problem. A tree-like data structure (Fig. 2a) enables *adaptive sparse grids* to develop a locally refined mesh where the solution requires it (cf. [5], [6]). We denote the weights of the finite elements in the approximation of the function $u(x)$ by $\tilde{u}_I$, i.e.

$$u(x) \simeq \sum_I \tilde{u}_I \tilde{v}_I(x)\,, \tag{1}$$

where $\tilde{v}_I(x)$ are the hierarchical basis functions. We now have a simple adaptation criterion which we can apply without external control over the adaptation process: if

$$|\tilde{u}_I| \stackrel{!}{>} \varepsilon_S \tag{2}$$

holds, the mesh is refined at the grid point with index I. As $|\tilde{u}_I|$ is generically small for small supports (i.e. functions towards the "leaves" of the tree), this process comes to an end when the refinement has developed sufficiently. A detail of an adaptive sparse grid around a singularity (Fig. 2b) illustrates the further reduction in the number of points compared to a regular sparse grid.

2.3.2 Shield Grids

As is obvious from Fig. 3, a hierarchical basis function, especially one with a large support, interacts with a large number of other finite elements (i.e. the intersection of the supports is not empty). This "non-local" character of sparse grids may lead to a spreading of local approximation errors over the domain. One would like to avoid this effect, e.g. if the potential has a

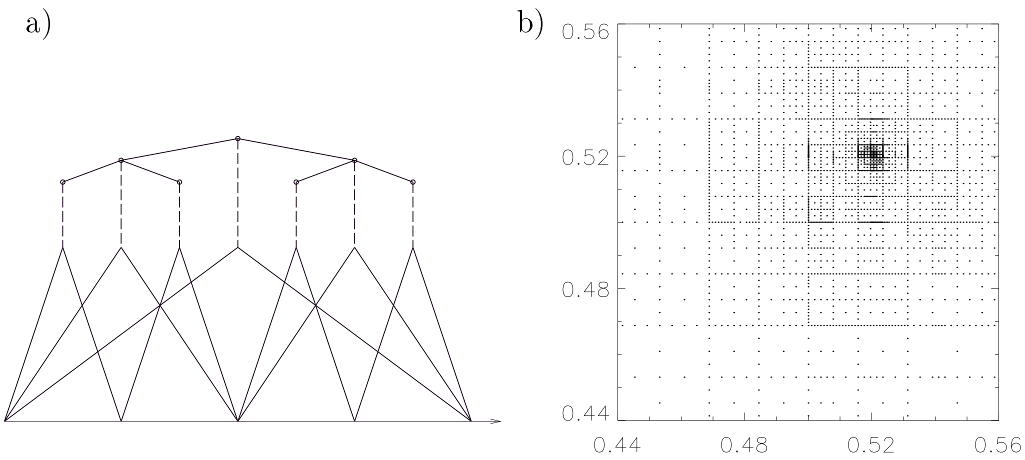

Figure 2: a) Tree scheme for one-dimensional hierarchical grids. b) Adaptive sparse grid.

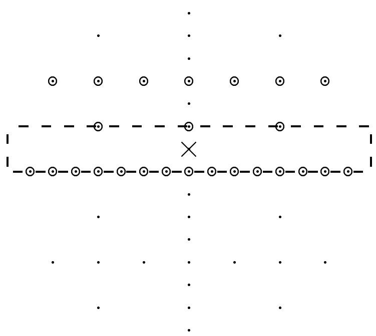

Figure 3: Non-locality in a hierarchical grid: the element with the dashed support ($\times$) has non-vanishing overlaps with all the $\circ$ elements.

singularity at some point, from which a large error could affect the whole solution. A sparse grid structure called a *shield grid*, located around the singularity, can keep the large errors localized, because all influences are compensated within a short distance. Fig. 4 shows an example of a shield grid. Its complexity is still that of a sparse grid.

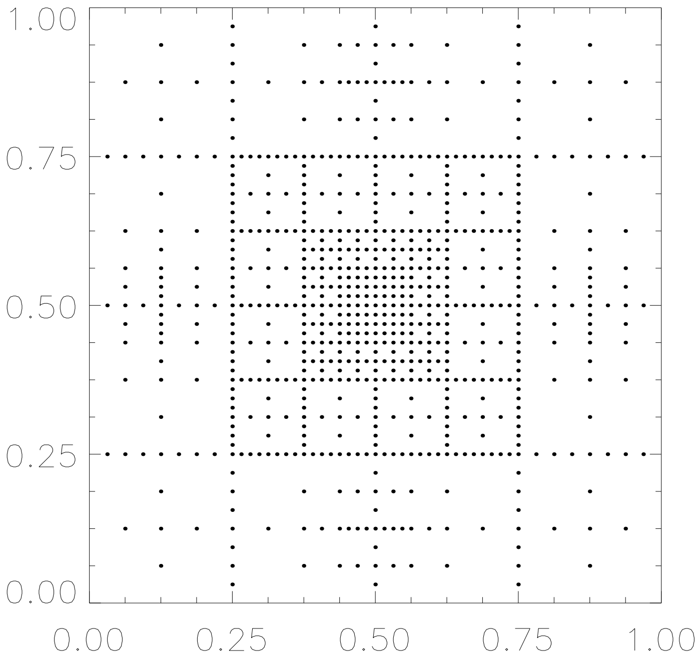

Figure 4: Two-dimensional shield grid.

3 Algorithms and Implementation

A Ritz-Galerkin method on rectangular sparse grids is used for solving stationary Schrödinger problems of dimensionality $D \geq 2$ in cartesian coordinates. We consider the (rescaled) Schrödinger equation

$$- \Delta u(\vec{x}) + V(\vec{x})\, u(\vec{x}) = E u(\vec{x}) \ , \ \vec{x} \in \Omega \equiv [0,1]^D \tag{3}$$

with potential function $V(\vec{x})$ and energy eigenvalue E using natural boundary conditions

$$u(\vec{x}) = 0 \quad \text{on} \quad \partial\Omega \ . \tag{4}$$

Eq. (4) is an excellent approximation to reality for any problem with localized probability densities and appropriate scaling of the integration domain. We will adopt this condition for all problems discussed, taking care that the approximation error resulting from (4) does not exceed the numerical errors of the FEM method.

Discretization leads to a generalized algebraic eigenvalue problem of the form

$$(L+P)\cdot\tilde{u} = E\cdot M\tilde{u}\ , \tag{5}$$

where the matrix elements are given by

$$\begin{aligned} L_{IJ} &\equiv \int_\Omega \langle\vec{\nabla}\tilde{v}_I, \vec{\nabla}\tilde{v}_J\rangle\, d^Dx\ , \\ P_{IJ} &\equiv \int_\Omega V(\vec{x})\ \tilde{v}_I\cdot\tilde{v}_J\, d^Dx\ , \\ M_{IJ} &\equiv \int_\Omega \tilde{v}_I\cdot\tilde{v}_J\, d^Dx\ . \end{aligned}$$

$\tilde{v}_I$ are piecewise D-linear hierarchical basis functions. $\tilde{u}$ is the approximation vector for the solution of (3).

(5) is solved by an inverse iteration (Wielandt) method (cf. [13]) that yields an improved approximation vector $\tilde{u}^{(n)}$ for the eigenvector in every iteration step (n), $n\in\mathbb{N}_0$, by solving the linear system

$$\Big(L+P-\bar{E}\cdot M\Big)\cdot\tilde{u}^{(n+1)} = \alpha^{(n)}\cdot M\tilde{u}^{(n)}\,. \tag{6}$$

$\alpha^{(n)}$ is a normalization value. $\tilde{u}^{(n)}$ converges to the eigenvector whose corresponding eigenvalue is nearest to a given seed value $\bar{E}$. The eigenvalue itself follows from an eigenvector approximation by a generalized Rayleigh quotient:

$$E^{(n)} = \frac{\tilde{u}^{(n)T}\,(L+P)\,\tilde{u}^{(n)}}{\tilde{u}^{(n)T}\,M\,\tilde{u}^{(n)}}\,. \tag{7}$$

For the solution of each linear system, a preconditioned conjugate gradient method is applied, using a multigrid-like approach for sparse grids [5], where the iteration uses additional residuals that can easily be computed by linear combination of residuals corresponding to the usual hierarchical basis functions.

Because of the different support sizes of hierarchical finite elements, the matrices P, M given in (5) are in general not sparse. A part of the improved complexity resulting from the reduction of the approximation space would be lost if all elements of these matrices had to be stored. However, with the help of algorithms decribed in [7] or [10] this can be avoided. Thus, the advantages of the sparse grid method can be fully exploited.

To obtain results for Schrödinger problems, the algorithms described were implemented into a C++ program called SGSS (*Sparse Grid Schrödinger Solver*). The computations were carried out on Hewlett-Packard workstations with $\leq$ 128 MB main storage capacity.

4 Numerical Results

This chapter will give eigenvalues and eigenfunctions for stationary one-particle Schrödinger problems as well as a system of Schrödinger equations. For most of the examples, solutions are known analytically, from perturbative computations or accurate numerics and can thus be used for evaluation of numerical errors. Every problem was computed regardless of possible reduction of its dimension by coordinate transformation or separation to demonstrate the advantages of sparse grids in high-dimensional applications. For a more detailed discussion of these results see [6].

4.1 Oscillator Potentials

Let us first consider anisotropic harmonic oscillator potentials, resulting in a Schrödinger equation of the form

$$-\Delta u(\vec{x}) + \kappa^2 \sum_{i=1}^{D} \left[\beta_i^2 (x_i - 0.5)^2\right] u(\vec{x}) = E \cdot u(\vec{x}) \quad , \quad \vec{x} \in [0,1]^D \, . \tag{8}$$

We chose the anisotropies β_i according to recent conventional FEM work ([14], [15]) to be able to compare them with our method. For the two-dimensional case, the sparse grid results are about two orders of magnitude more accurate (with respect to eigenvalues) than the values of these authors with the same number of points and basis functions of the same order (cf. Fig. 5). The exact solutions are, of course, known from analytical computations.

As an example for a excited state eigenfunction, we present a state with quantum nubers $n_1 = 0, n_2 = 2$ in Fig. 6. It is noteworthy that the accuracy of the corresponding eigenvalue does not fall behind that of the ground state value.

Isotropic and anisotropic harmonic oscillators are solved with good accuracy in up to 5 dimensions. With errors of about 10^{-2} in the eigenvalue, computations up to $D = 8$ are possible.

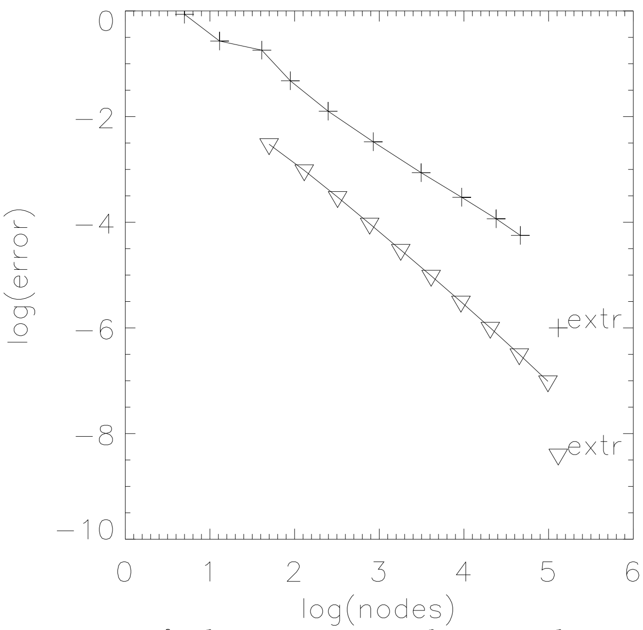

Figure 5: Comparison of relative errors in the ground state energy of a two-dimensional anisotropic harmonic oscillator, plotted vs. the number of nodes (decadic logarithm on both axes). + signs: [15] (adaptive full grids); ▽ signs: this work (regular sparse grids). Both computations use first order finite elements. Also shown are the respective extrapolated values.

Results for anharmonically perturbed two-dimensional oscillators, i.e. for a potential

$$V(\vec{x}) = \kappa^2(r^2 + r^4), \quad r^2 \equiv \sum_{i=1}^{D}(x_i - 0.5)^2, \quad \vec{x} \in [0,1]^D \;, \tag{9}$$

are of the same quality as for the harmonic problems (this can be demonstrated by using high-order perturbation theory, cf. [6]), thus showing that properties like separability or symmetries do not play a significant role for the accuracy of the sparse grid FEM.

The use of adaptive sparse grids instead of regular sparse grids does not seem to yield overwhelming progress for these kinds of problems. Nevertheless, in 3 dimensions, adaptive grid computations tend to be more accurate than those on regular grids (see [6]).

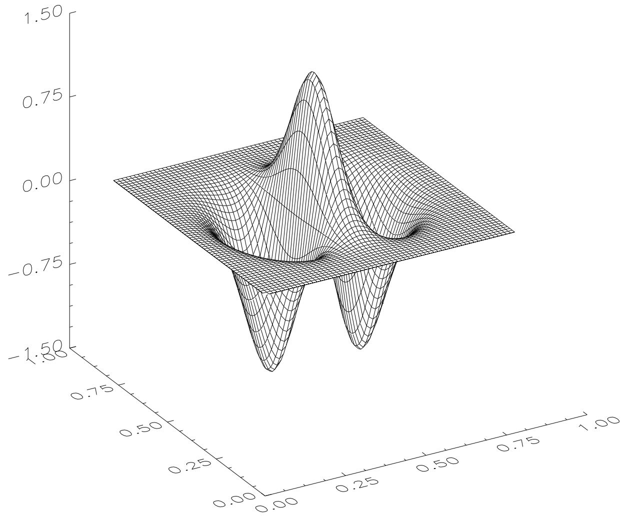

Figure 6: $(n_1 = 0, n_2 = 2)$ state of the anisotropic harmonic oscillator; regular sparse grid (20481 nodes), relative error of the eigenvalue: $\delta E = -1.28 \cdot 10^{-6}$.

4.2 Singular Problems

Reasonable accuracy was also achieved for problems with singular potential in three dimensions, viz the hydrogen atom and the hydrogen molecular ion. In these cases, the use of adaptive and/or shield grids is of eminent importance (cf. sections 2.3.1 and 2.3.2). Again, none of the calculations exploits inherent symmetries of the problems; similar accuracy is to be expected for arbitrary potentials.

As an example, we show in Fig. 7 a $3s$ eigenfunction of the (non-relativistic) hydrogen atom. The calculation was carried out on a 3D adaptive sparse grid. The potential that has to be inserted in the Schrödinger equation (3) is the Coulomb potential, whose strength is characterized by a positive constant κ (proportional to the charge of the atomic core):

$$V(\vec{x}) = -\kappa \frac{1}{r}, \quad r^2 \equiv \sum_{i=1}^{3} (x_i - 0.5)^2 \;, \tag{10}$$

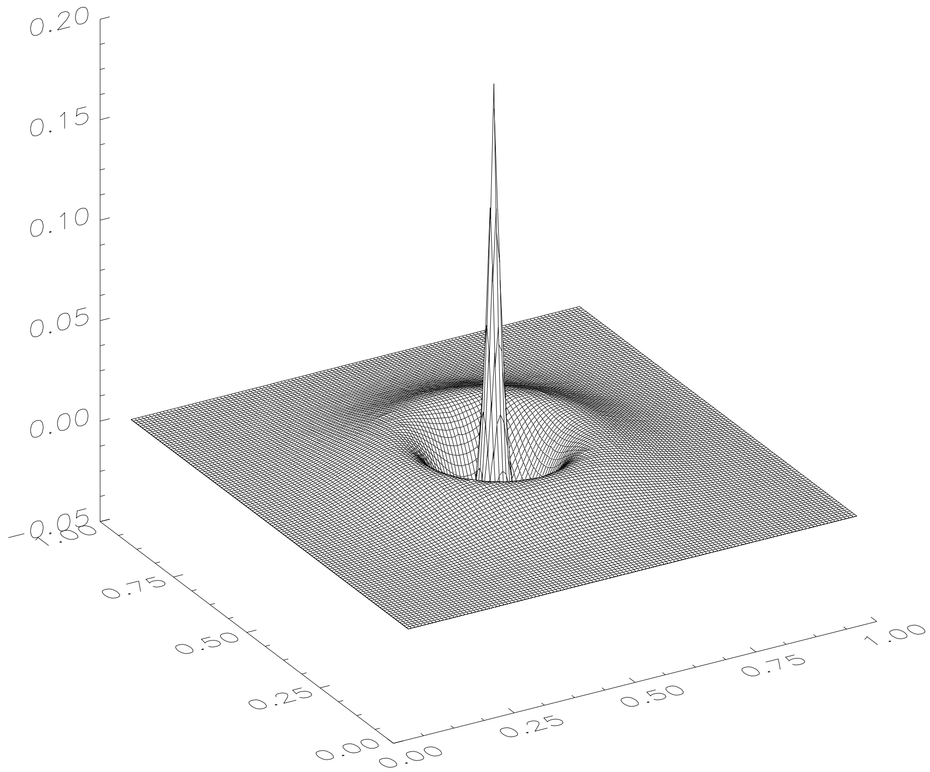

Figure 7: $3s$ state of the hydrogen atom; adaptive sparse grid (105619 nodes), $\varepsilon_S = 1 \cdot 10^{-2}$, $\delta E = 5.68 \cdot 10^{-3}$.

We also calculated ground states and excited states of a hydrogen molecular ion (H_2^+) in Born-Oppenheimer approximation. The potential consists of two Coulomb singularities within a distance $|\vec{d}\,|$ of 2 a.u.[1] of each other:

$$V(\vec{x}) = \kappa \left(-\frac{1}{|\vec{r}-\vec{d}|} - \frac{1}{|\vec{r}+\vec{d}|} \right), \quad r^2 \equiv \sum_{i=1}^{D} (x_i - 0.5)^2, \quad \vec{x} \in [0,1]^D \ . \quad (11)$$

[1] *atomic units* are common in atomic and molecular physics; the unit of length is Bohr's radius $a_B \simeq 0.0529$ nm

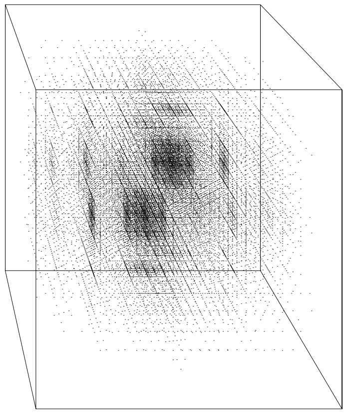

Figure 8: Perspective view of the nodes of an adaptive sparse grid for the problem of the H_2^+ ion (22239 points).

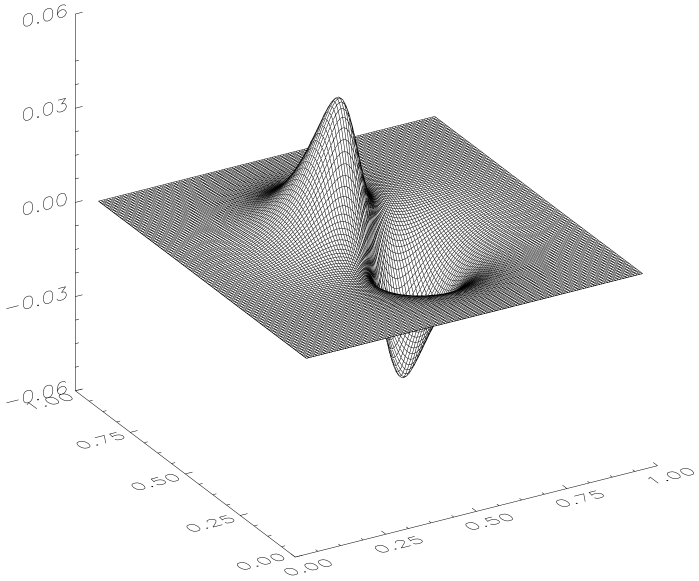

Figure 9: Excited ($1\sigma_u$) state of the H_2^+ ion; adaptive sparse grid (54433 nodes), $\kappa = 25$, $\delta E = 8.15 \cdot 10^{-4}$.

Fig. 8 shows a typical adaptive sparse grid generated by the program SGSS for this problem. As expected, nodes are highly concentrated around the two singularities.

We give an excited ($1\sigma_u$) state in Fig. 9. Note that this section of the function does not include the singularities, which is why no "spikes" are visible. The accuracies obtained in the case of singular potentials are not as high as for oscillator-like potentials. There is, however, no example for a 3D calculation using piecewise multilinear elements for singular potentials with an accuracy as high as a few 10^{-4}. Also, there is no obstacle in principle to implement higher order finite elements into the sparse grid algorithm (this has already been done for bicubic functions in [11]).

4.3 Spin Boson Coupling

New calculations show that the sparse grid FEM is also able to solve systems of Schrödinger equations very efficiently. A simple spin boson coupling model (cf. [16]) with the Hamiltonian

$$H \begin{pmatrix} \psi \\ \phi \end{pmatrix} = \begin{pmatrix} H_{osc}(\kappa_i^{(+)}, E^{(+)}) & g \\ g & H_{osc}(\kappa_i^{(-)}, E^{(-)}) \end{pmatrix} \begin{pmatrix} \psi \\ \phi \end{pmatrix} \tag{12}$$

describes the coupling of a two state system (e.g. electron spin) to D continuous degrees of freedom (harmonic oscillators), i.e. ψ and ϕ are functions of $\vec{x} \equiv (x_1, \ldots, x_D)$. This constitutes a simple model for various systems and phenomena, e.g. electronically excited molecules, vibronic coupling, Jahn-Teller effect etc. The centers of the oscillators are displaced from the origin along the x_i-axis by the values $\kappa_i^{\pm}$ and along the energy axis by $E^{\pm}$. Thus, $H_{osc}(\kappa_i^{\pm}, E^{\pm}) \equiv \sum_i \left\{ p_i^2 + (x_i - \kappa_i^{\pm})^2 \right\} + E^{\pm}$.

This problem is not solvable by analytical techniques; conventional numerical calculations rarely go beyond $D = 5$. SGSS could compute ground state eigenvalues for D up to 8. These calculations were carried out on workstations and without grid adaptation, which would have yielded further gain in effectiveness. Fig. 10 shows the components ψ and ϕ of the eigenvector for the aforementioned ground state in 8 dimensions. In Fig. 11 we present a higher eigenstate of the 2-dimensional problem, with a considerable shift $E^{\pm}$ on the energy axis.

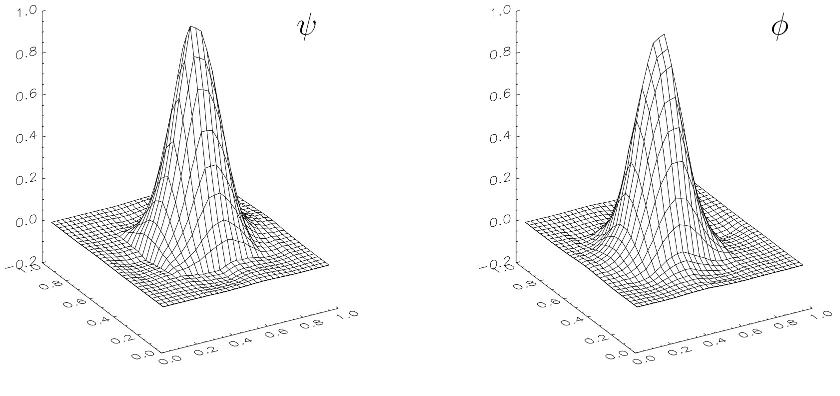

Figure 10: Ground state functions of the 8-dim. spin boson coupling problem with arbitrarily chosen $\kappa^+ = -\kappa^- = (0.1, 0.05, 0.033, 0.066, 0.01, 0, 0.05, 0)$, $E^{\pm} = 0$. Regular sparse grid (31745 nodes).

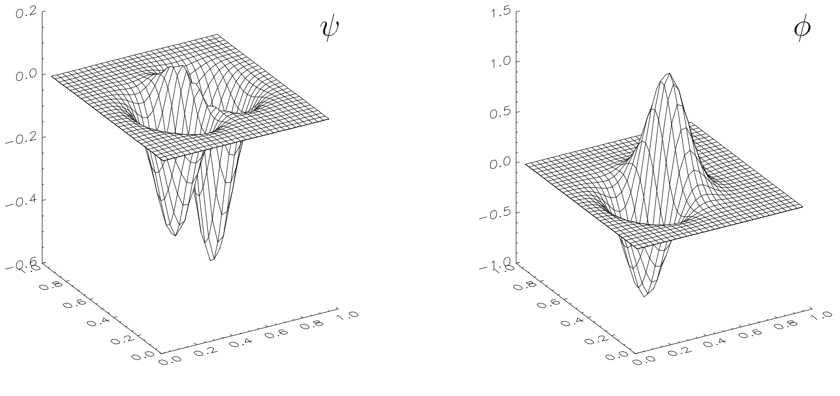

Figure 11: An excited state of the 2-dim. spin boson coupling problem. $E^+ - E^- \simeq 0.1E$, $\kappa^+ = -\kappa^- = (0.1, 0.05)$. Regular sparse grid (20481 nodes)

5 Summary, Conclusions

Sparse grid methods are able to solve stationary Schrödinger equations with smooth potential functions with far greater accuracy than conventional FEM. The use of adaptive sparse grids allows for automatical refinement of the grid where smaller mesh widths are needed, e.g. around a singularity of the solution. Recent computations on systems of Schrödinger equations show that this method is probably the first that allows for highly accurate computations of almost arbitrary problems in more than 6 dimensions. Applications in various fields of physics (e.g. molecular quantum physics, solid state physics or hydrodynamics [12]) are numerous.

Future work should concentrate on the implementation of higher order basis functions and new differential terms into the equation. As time-dependent problems are have already been treated with sparse grids [8], it is also straightforward to modify the algorithm in order to solve the time-dependent Schrödinger equation. Modeling scattering events or the dynamics of molecular reactions appear to be promising fields of application for this method. The latter kind of problem requires including multi-particle terms into the equation or, if applied to a large number of degrees of freedom, implementation of approximations like Hartree-Fock. Although these modifications might demand more programming skill than in conventional programs, they should not pose an unsolvable problem.

Since accuracy is expected to rise dramatically once higher order sparse grid elements are applied, we are confident to state that for Schrödinger problems, implementation of sparse grid methods with finite element functions of higher order will likely lead to extremely powerful tools.

References

[1] H. Yserentant, *On the multi-level splitting of finite element spaces*, Numerische Mathematik **49**, 379 (1986).

[2] C. Zenger, *Sparse grids*, in *Parallel Algorithms for Partial Differential Equations: Proceedings of the Sixth GAMM-Seminar, Kiel, 19.1.–21.1. 1990*, edited by W. Hackbusch, *Notes on Numerical Fluid Mechanics* (Vol. 31), Vieweg, Braunschweig, (1991).

[3] C. Zenger, *Hierarchische Datenstrukturen für glatte Funktionen mehrerer Veränderlicher* in Informatik und Mathematik , M. Broy, Hrsg., Springer (1991).

[4] M. Griebel, *Zur Lösung von Finite-Differenzen- und Finite-Element-Gleichungen mittels der Hierarchischen-Transformations-Mehrgitter-Methode*, Technische Universität München, Dissertation (1990).

[5] M. Griebel and P. Oswald, *On additive Schwarz preconditioners for sparse grid discretizations*, Friedrich-Schiller-Universität Jena, Forschungsergebnisse der mathematischen Fakultät (1992).

[6] S. Hilgenfeldt, *Numerische Lösung der stationären Schrödingergleichung mit Finite-Element-Methoden auf dünnen Gittern*, Diplomarbeit, Technische Universität München, Institut für Theoretische Physik und Institut für Informatik (1994).

[7] H.-J. Bungartz, *Dünne Gitter und deren Anwendung bei der adaptiven Lösung der dreidimensionalen Poisson-Gleichung*, Technische Universität München, Dissertation (1992).

[8] R. Balder, *Adaptive Verfahren für elliptische und parabolische Differentialgleichungen auf dünnen Gittern*, Dissertation am Institut für Informatik der Technischen Universität München (1994).

[9] S. Hilgenfeldt, R. Balder, and C. Zenger, *Numerical Solution of the Stationary Schrödinger Equation using Finite Element Methods on Sparse Grids*,to appear in *J. Comput. Phys.*

[10] R. Balder and C. Zenger, *The solution of the multidimensional Helmholtz equation on sparse Grids*, to appear in: SIAM J. of Sci. Comp.

[11] T. Störtkuhl, *Ein numerisches Verfahren zur Lösung der biharmonischen Gleichung auf dünnen Gittern*, Dissertation am Institut für Informatik der Technischen Universität München (1994).

[12] M. Griebel, W. Huber, C. Zenger, *A fast Poisson solver for turbulence simulation on parallel computers using sparse grids*, in: E.H. Hirschel (Hrsg.), *Flow Simulation with High-Performance Computers I, Notes on Numerical Fluid Mechanics*, Vieweg (1993).

[13] G. Peters and J. H. Wilkinson, SIAM J. Numer. Anal. **7**, 479 (1970).

[14] J. R. Alvarez-Collado and R. J. Buenker, J. Comp. Chem. **13**, 135 (1992).

[15] J. Ackermann and R.Roitzsch, Chem. Phys. Lett. **214**, 109 (1993).

[16] A. J. Leggett, S. Chakravarty, A. T. Dorsey, M. P. A. Fisher, A. Garg, and W. Zwerger, Rev. Mod. Phys. **59**, 1 (1987).